Available online at www.sciencedirect.com
ScienceDirect
Acta Materialia 56 (2008) 3791–3799
Acta MATERIALIA
www.elsevier.com/locate/actamat

Full-field strain evolution during intermartensitic transformations in single-crystal NiFeGa

C. Efstathiou [a], H. Sehitoglu [a,*], J. Carroll [a], J. Lambros [a], H.J. Maier [b]

[a] University of Illinois at Urbana Champaign, Department of Mechanical Science and Engineering, 1206 West Green Street, Urbana, IL 61801, USA
[b] University of Paderborn, Lehrstuhl f. Werkstoffkunde, D-33095 Paderborn, Germany

Received 6 November 2007; received in revised form 4 April 2008; accepted 7 April 2008
Available online 18 May 2008

Abstract

Using in situ digital image correlation to obtain full-field measurements, we study the intermartensitic transformations in single-crystal NiFeGa. Full-field strain measurements identify the coexistence of modulated martensite phases during the first plateau of the multistage stress–strain curve at room temperature. At a higher temperature, the measurements indicate the bypassing of one of the modulated phases. Strain as high as 13% is measured as a result of the transformation to the intermediate monoclinic modulated and final tetragonal phase. Based on the full-field strain measurements, the phase fractions during the nucleation and the progression of the transformation are obtained. The evolution of the local strain and the phase fractions prove critical in explaining strain softening, hysteresis and other phenomena observed in the stress–strain curves.

Keywords: Digital image correlation; Nucleation of phase transformations; Martensitic transformation; Metastable phases; Shape memory alloy (SMA)

1. Introduction

Martensitic transformations have been a topic of significant scientific and technological interest. The reversibility of the martensitic transformation in shape memory alloys (SMAs) has been exploited in engineering applications ranging from actuation, sensing, and medical devices, mostly with the use of NiTi-based alloys with recoverable strains usually less than 6%. Several emerging SMAs exhibit multiple martensitic transformations or intermartensitic transformations with large recoverable strains (>10%). Due to intermartensitic transformations, these materials display intricate stress–strain curves with multiple plateaus and abrupt stress drops that are not easily understood with conventional experimental techniques.

In previous studies, researchers inferred the formation of different martensitic phases by means of indirect evidences, such as comparison of the plateau strain with theoretical values [1–4]. The premise of this approach is that the measured plateau strain corresponds to the theoretical strain of a single transformation, and assumes the entire material volume completely transforms. Potential drawbacks of this approach arise when multiple transformations occur over a single plateau or when a transformation is incomplete. When multiple transformations occur over a single plateau such as in NiFeGa, the plateau strain measured with an extensometer may no longer agree with the theoretical transformation strain because the extensometer effectively averages the contribution of each martensite. To circumvent this difficulty, we utilize digital image correlation (DIC) to obtain full-field strain measurements. The full-field strain measurements are used to identify each martensite phase independent of the plateau strain.

Recent investigations have identified that intermartensitic transformations result in a multistage stress–strain curve with two plateaus in NiFeGa when loaded in tension at room temperature [3–6]. Sutou et al. [3] reported that the intermartensitic transformation sequence at room temperature is $A \rightarrow 14M \rightarrow L1_0$ for a [1 0 5] oriented NiFeGa

* Corresponding author. Tel.: +1 217 333 4112; fax: +1 217 244 6534.
E-mail address: huseyin@uiuc.edu (H. Sehitoglu).

1359-6454/$34.00
doi:10.1016/j.actamat.2008.04.033

crystal whereas Hamilton et al. [4] reported $A \rightarrow 10M \rightarrow 14M \rightarrow L1_0$ for a [0 0 1] oriented crystal of the same nominal composition. These reported transformation sequences occur under stress and are inferred from local strain measurements. In our previous work, the extra reflections observed in selected area diffraction patterns have directly identified the 10M and 14M martensites due to thermal cycling [4]. Since these previous investigations relied on the plateau strain measurement to determine the transformation sequence, it is of interest to clarify the apparent discrepancy using local strain measurements. In the current work, local strain measurements are obtained in situ during the intermartensitic transformations in NiFeGa. The full-field measurements allow the transformation sequence and the relative amount of each phase to be determined during loading and unloading.

Previous studies have also investigated the transformation behavior of NiFeGa at higher temperatures (50–125 °C) and noted a stress–strain curve with a drastic stress drop and a single plateau [3,4]. The plateau strain measurements obtained by Sutou et al. indicated the $A \rightarrow L1_0$ transformation occurred over the plateau, but they speculated that this transformation could not occur without the nucleation of the 14M phase. The results obtained by Hamilton et al. inferred that the $A \rightarrow 14M \rightarrow L1_0$ transformation occurred over the plateau. However, no direct measurements or descriptions have been reported to verify the proposed 14M intermediate phase in NiFeGa. The measurements presented in this paper will verify the proposed intermediate 14M phase, and describe its evolution.

Recently, local strain measurements were made in polycrystalline NiTi using DIC [7]. DIC is a real-time and full-field optical technique used to measure surface deformations. This previous study and many others utilizing different techniques [8–14] have focused on polycrystalline NiTi alloys where the stress–strain response is influenced by the distribution of stresses, strains, grain orientations, and phase fractions within grains [15]. In contrast to polycrystals, the study of single-crystals permits the multistage transformation to be interrogated without the influence of grain boundaries; consequently, the nucleation of transformation fronts from soft grains or from grain boundaries can be ruled out. In this paper, the focus on single-crystals with the use of DIC also permits the phase fraction, and the heterogeneity of the transformation, to be directly determined and related to the stress–strain and hysteresis behavior.

In regard to stress-induced intermartensitic transformations in single-crystal NiFeGa, this paper, using DIC measurements, will: (i) clarify which intermartensitic transformations occur at room temperature, (ii) verify and describe the proposed transformation sequence at a higher temperature, (iii) explore possible explanations for transformation strains not reaching theoretical strain levels. The current work is the first investigation utilizing DIC techniques to gain a more precise understanding of the role of external stress and temperature on intermartensitic transformations which involves phase boundary motion, transition layers, and the evolution of phase fractions.

2. Experimental techniques

The alloy of interest was cast to a nominal composition of $Ni_{54}Fe_{19}Ga_{27}$ (at.%). Single-crystals were grown using the Bridgman technique in an inert environment. The forward and reverse transformation temperatures (peaks of differential scanning calorimetry curves) were determined as 0 °C and 16 °C, respectively [16]. Small-scale dog-bone-shaped specimens with a 1.5 mm × 3 mm cross-section and a 10 mm gage length were electro-discharged-machined with their loading axis along the [0 0 1] crystallographic direction. Uniaxial tensile experiments were conducted at 22 °C and 50 °C, which are both above the reverse transformation temperature. Thus, the stress–strain response was completely pseudoelastic. Experiments were conducted under strain control or position control.

To gain an understanding of the stress–strain response with intermartensitic transformations it is illustrative to study Fig. 1. Pseudoelasticity is defined as the total recovery of deformation during unloading, albeit with hysteresis. Research on martensitic transformations in NiFeGa alloys has shown that the ordered $L2_1$ austenite (A) structure transforms to martensite phases designated as 10M, 14M, and $L1_0$ depending on the applied stress state and temperature [4]. The sequence of these transformations was described as $A \rightarrow 10M \rightarrow 14M \rightarrow L1_0$ for a [0 0 1] oriented crystal loaded in tension at room temperature [4]. The first plateau stage in Fig. 1 contains the $A \rightarrow 10M \rightarrow 14M$ forward transformation and the $14M \rightarrow 10M \rightarrow A$ reverse transformation. The second plateau stage contains the $14M \rightarrow L1_0$ forward transformation and the $L1_0 \rightarrow 14M$ reverse transformation. At higher temperatures, only one plateau stage is observed and the forward transformation sequence becomes $A \rightarrow 14M \rightarrow L1_0$ (not shown). Details of the crystallography of the intermartensitic transformations are reported in Ref. [4].

In situ macroscopic observations were used to investigate the evolution of the transformation. Images were captured with an IMI model IMB-202FT CCD camera (1600 pixels × 1200 pixels). A Navitar optical lens was used for macroscopic observations at low magnification which resulted in a resolution of 135 pixels mm^{-1}. DIC was performed on images of approximately 1.6 mm × 5 mm regions of interest to determine the local strain fields during loading and unloading. Full-field measurements of both in-plane displacement components are obtained using DIC. The DIC technique measures displacement fields by tracking features on the specimen surface with a random speckle pattern [17]. Speckle patterns were applied to the surface of polished specimens using an Iwata Micron B airbrush. To perform DIC, a region of interest is selected in the reference image and divided into small square regions called subsets. Each subset represented a square region

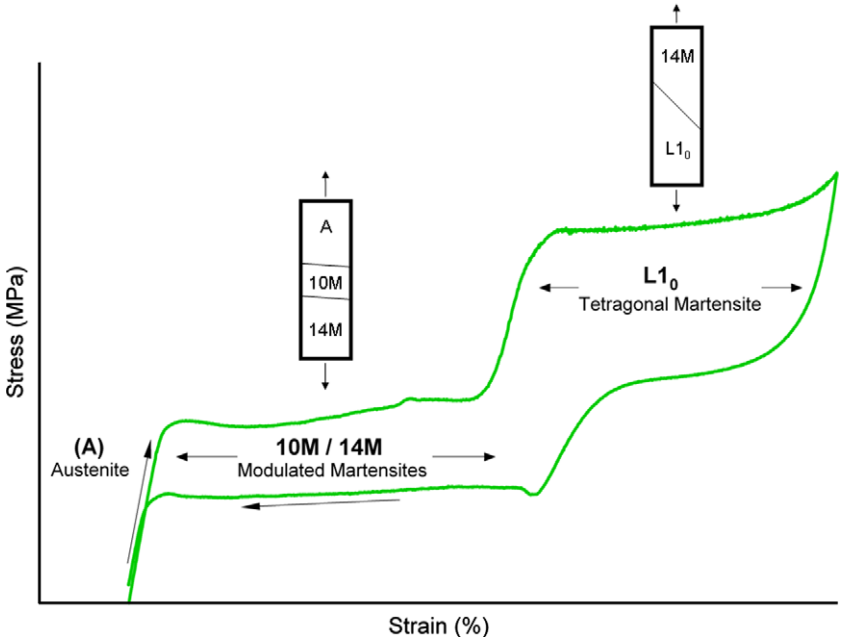

Fig. 1. A schematic of the pseudoelastic stress–strain curve of NiFeGa showing the multiple plateau stages observed at room temperature. The associated martensite phases are identified over each plateau stage. The austenite has an ordered $L2_1$ type crystal structure, the 10M and 14M are modulated monoclinic martensites, and the $L1_0$ is a tetragonal martensite.

approximately 200 μm × 200 μm. Approximately 17 000 subsets were used to create the strain fields presented. The average pixel intensity in each subset is calculated, and regions with the same intensity are sought in the deformed image. In order to find the location of a deformed subset and its shape change, optimization techniques are employed in which values of displacement and linear displacement gradients of a subset are obtained. For each subset, these values are adjusted until the difference in pixel intensity between the reference and deformed subsets is a minimum. The resulting displacement field is then differentiated to obtain the strain field according to a central difference scheme. The nominal strain was calculated by averaging the DIC strain field. Including higher-order displacement gradients had an insignificant effect on the results. The strain fields are subsequently used to determine the fraction of each phase. This is done by comparing the measured strain to theoretical values of strain having accounted for an approximate elastic strain and the transition region between the two phases. Commercially available software (Vic2d) from Correlated Solutions was used to perform the image correlation and the strain calculations. Further details on the application of DIC can be found in Ref. [17] and a general background on DIC is given in [18].

3. Experimental results

Fig. 2 displays the nominal stress–strain curve at room temperature and the corresponding DIC strain fields. An animation of the local strain field with the evolution of the stress–strain curve is provided in Supplementary Video 1 to illustrate thoroughly the transformation sequence that is subsequently discussed. Upon tensile loading, the initial local strain is homogeneous as shown by the single dark purple image. A sequence of ten images corresponding to the ten marker points illustrates the local strain measured during the first plateau. In the second image of the sequence (left to right), the strain field indicates the nucleation of a band (blue region)[1] with approximately 4% strain. The nucleation of this band occurs at the onset of the critical transformation stress, and propagates while the stress–strain curve exhibits a slight strain softening. This 10M band propagates along the specimen length with a relatively constant width. Before this transformation is complete, another region (green color) develops with approximately 6% strain. The local strain measurements in the "blue" and "green" regions correspond to theoretical transformation strains for the 10M (4.6%) and 14M (6.2%) phases, respectively [3]. At room temperature, the 10M phase always precedes the 14M phase. The strain fields in these two regions provide, for the first time, direct evidence of the coexistence of the 10M and 14M phases in the first plateau stage.

At approximately 5% nominal strain, a second stress peak is observed. This peak is not due to a nucleation event in contrast to the first critical transformation stress peak. The phenomenon controlling the occurrence of the second stress peak will be elaborated on in a later section.

[1] For interpretation of color in Figs. 2–4, the reader is referred to the web version of this article.

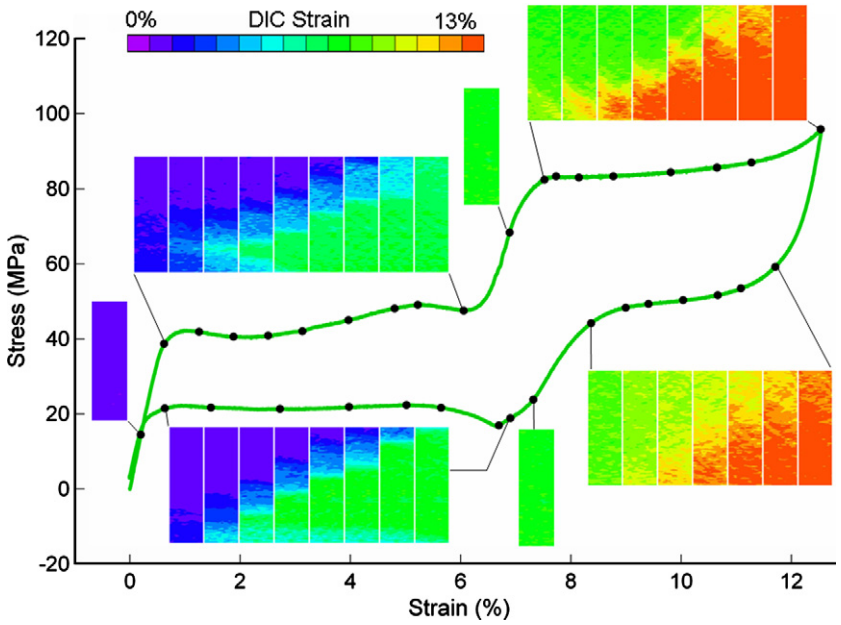

Fig. 2. The nominal stress–strain curve at room temperature, and the strain fields obtained using DIC at selected points along the curve. A total of 35 strain fields are shown each corresponding to a solid black marker on the stress–strain curve. The loading axis for all strain fields is vertical, and the color contours represent magnitudes of axial strain in a common scale. The strain fields correspond to a 1.6mm × 5 mm region of the tensile sample.

At the end of the first plateau, the entire gage section has transformed to the 14M phase and a marked increase in stiffness occurs. The local strain field indicates a region of homogeneous deformation until the critical transformation stress for the second plateau stage is achieved at approximately 80 MPa. The sequence of eight images in the upper right of Fig. 2 displays the initiation and propagation of the forward transformation during the second plateau. The local strain shown as a red region (12.2–13% DIC strain) corresponds to the theoretical transformation strain for the $L1_0$ phase [3]. The $L1_0$ phase transforms primarily as a single front, but shows multiple fronts by 9% nominal strain (see the fifth image of the upper right image sequence). These fronts represent different correspondent variant pairs (CVPs) as is indicated by their different inclination angle (+45° and −45°) to the loading axis. At the conclusion of the loading, the entire area of observation has transformed to the $L1_0$ phase.

The straining direction is then reversed resulting in an elastic unloading portion of the stress–strain curve with homogeneous deformation. At about 50 MPa, a plateau associated with the reverse transformation begins. The image sequence in the lower right of Fig. 2 shows the strain fields during the reverse transformation. The most notable feature of the strain fields during unloading of the second plateau stage is the diffuse interface and the homogeneous type nucleation (note the yellow patches dispersed within the red and green domains). By homogeneous nucleation we refer to multiple nucleation sites, and by heterogeneous nucleation we refer to nucleation during front propagation. After the completion of the $L1_0 \rightarrow 14M$ intermartensitic transformation, another region of homogeneous deformation with an increase in stiffness occurs. Then the $14M \rightarrow 10M \rightarrow A$ transformation commences heterogeneously by the propagation of a front. The front propagates in a reverse manner, which nearly mirrors the transformation during loading. This is illustrated by comparing the upper left sequence ($A \rightarrow 10M \rightarrow 14M$) to the lower left sequence ($14M \rightarrow 10M \rightarrow A$). The evolution of the local strain indicates that during loading the transformation occurs by heterogeneous type nucleation, whereas during unloading, the second plateau stage appears to be more homogeneous type nucleation, and the first plateau stage occurs by heterogeneous type nucleation.

To investigate the intermartensitic transformations further, we studied the tensile stress–strain response at 50 °C (Fig. 3). This loading temperature is considerably higher than the reverse transformation temperature and thus serves to stabilize the austenite structure. At 50 °C, the two-stage stress–strain curve is not observed. Instead, a single plateau is recorded after a drastic stress drop at the critical transformation stress of approximately 160 MPa. The DIC local strain measurements indicate that two distinct phases form after the stress drop. The first phase is identified by the green region with approximately 6% strain, and the second phase is identified by the red region with approximately 13% strain. Based on the theoretical transformation strains mentioned previously, the strain in these regions correspond to the 14M and the $L1_0$ martensites, respectively. Thus the transformation sequence identified by the local strain is $A \rightarrow 14M \rightarrow L1_0$. Note that as the transformation propagates, the 14M phase (green region) fraction remains a constant width while the $L1_0$ phase (red region) fraction increases until the entire gage section has transformed. This result is noteworthy because it shows the presence of the 14M phase preceding the $L1_0$ phase as

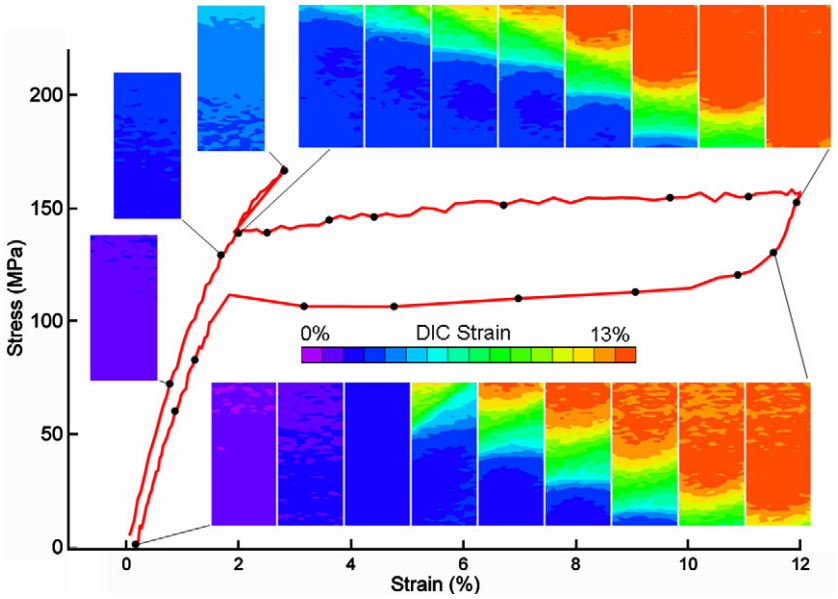

Fig. 3. The nominal stress–strain curve at 50 °C and the strain fields showing that the 10M transformation is bypassed, and a single plateau stage corresponding to the A → 14M → $L1_0$ transformation. The strain fields correspond to a 1.6 mm × 3.3 mm region of the tensile sample.

was proposed in Refs. [3,4], and it also identifies that a significant 14M phase fraction accompanies the $L1_0$ transformation.

An example of coexisting phases and the strain variation across their interfaces is presented in Fig. 4. The data plotted in this figure represent a line scan along the inset DIC image. Note that the loading axis for these DIC images is in the horizontal direction. The strains reported on the *y*-axis have had approximate elastic strains subtracted. In Fig. 4a, the two DIC images represent strain fields captured near the middle of the first and second plateau at room temperature. Two narrow transition regions are evident in the red curve. The first is between the A and 10M phase and the second is between the 10M and 14M phase. In both transformed regions the phases form interfaces that are inclined 3–6° to the applied tensile load. On the other hand, for the second plateau, the blue curve indicates a considerably wider transition width for the 14M → $L1_0$ transformation, and the interface is inclined at approximately 45° to the applied tensile load. For this relatively large transition width, the optical resolution is sufficient to describe the strain variation within the interface, and it appears to vary linearly.

At 50 °C, in Fig. 4b, the A → 14M → $L1_0$ transformations occurs over a short distance, and therefore each phase is outlined with a box to separate the two transition regions. The transition width between the A and 14M phase, and between the 14M and $L1_0$ phase, is similar to that observed at room temperature for the respective transformations. In the inset DIC image, the interface between A and 14M is inclined 3–6° to the applied load whereas the interface between the 14M and $L1_0$ phase appears curved. The curved interface is most likely due to a superposition of two habit planes inclined +45° and −45° to the applied load.

Comparing the measured transformation strains to the theoretical transformation strains (horizontal lines in Fig. 4a and b), it is apparent that only the 14M phase agrees well whereas the 10M and $L1_0$ phases appear smaller by approximately 1–2% strain. In all transformed regions, except for the 14M phase at 50 °C, the strains appear relatively uniform, and the transition regions exhibit a linear variation in strain.

For the purpose of measuring the phase fraction, midpoints of the transition regions described in Fig. 4 are chosen to identify which phases are present. At room temperature, in Fig. 5a, the phase fraction is shown as the nominal strain increases. First note that three phases (A, 10M and 14M) contribute to the total fraction over the first plateau whereas only two phases exist in the second plateau. Over the first plateau, the 10M phase fraction remains relatively constant while the austenite fraction decreases and the 14M phase increases linearly. Some nonlinearity in the phase fraction evolution is notable during the nucleation events which occur approximately between 0.5 and 1.2% strain.

At 50 °C in Fig. 5b, the 14M phase fraction remains approximately constant, while the austenite fraction decreases and the $L1_0$ fraction increases linearly. Again, some nonlinearity is notable during the transformation nucleation which occurs approximately between 1.7% and 3.0% in Fig. 5b. Although not shown, all trends are similar during unloading at both temperatures.

4. Discussion of results

The present approach circumvents plateau strain measurement difficulties and provides more conclusive evidence on the transformation sequence during intermartensitic transformations. The local strain measurements in Fig. 2

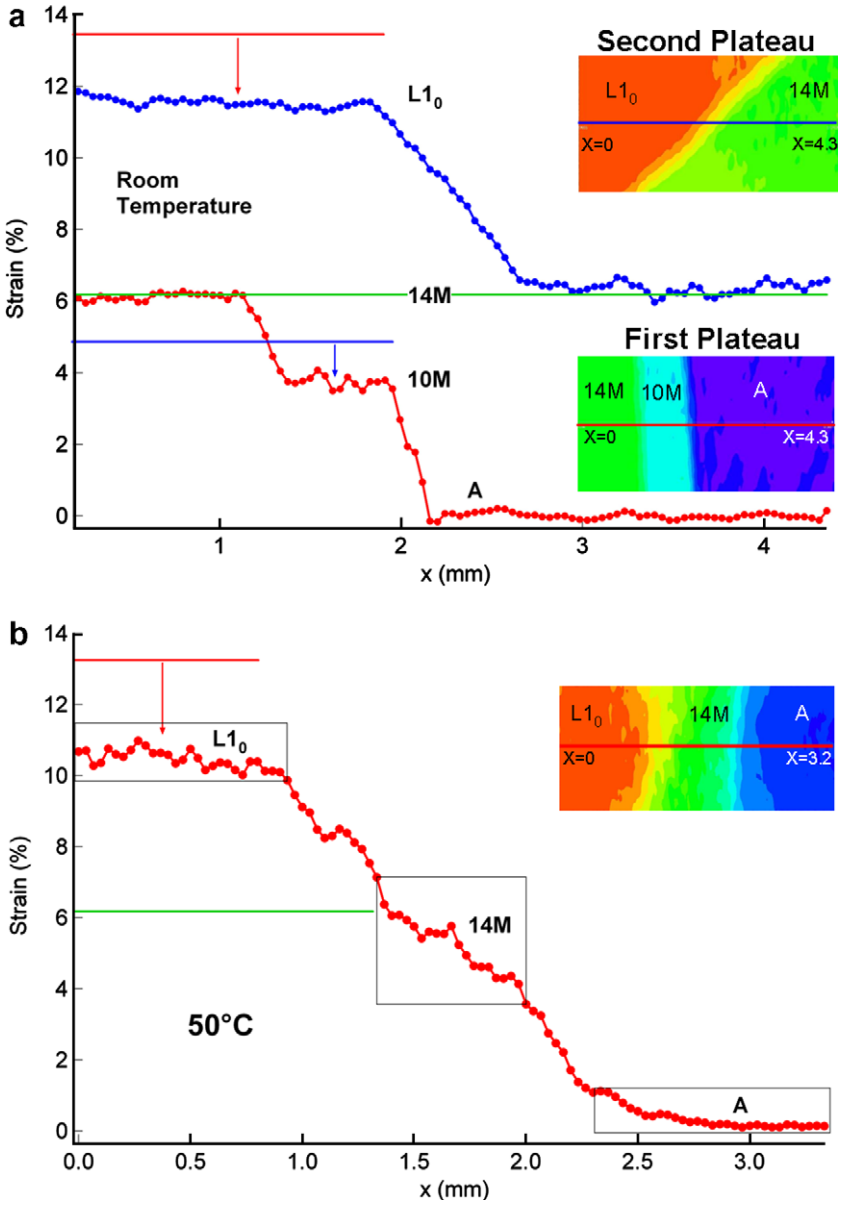

Fig. 4. Strain measurements along the line scan in the DIC image inset: (a) at room temperature, (b) at 50 °C. Note that these measurements have approximate elastic strains subtracted from the total strain to facilitate a comparison with theoretical strains shown by the horizontal lines.

have clarified the coexistence of 10M and 14M phases during the first plateau in [0 0 1] oriented single-crystal NiFeGa. These phases form sequentially, i.e. first approximately 35% of the volume undergoes the intermediate A → 10M transformation, and then the remainder undergoes the 10M → 14M transformation. Thus, the A → 10M → 14M transformation sequence over the first plateau confirms a previous postulate by Hamilton et al. [4].

It has also been proposed that at higher temperatures the $L1_0$ phase is stress-induced from austenite via an intermediate transformation to the 14M phase, and the resulting transformation sequence should be A → 14M → $L1_0$ [3]. This was anticipated because the formation of an undistorted plane between austenite and the $L1_0$ crystal structure would be more easily accommodated via the 14M structure since it includes high-density microtwins and an ordered stacking structure [3]. Examination of the local strain measurements at 50 °C in Fig. 3 verifies that the 10M transformation is bypassed allowing the A → 14M → $L1_0$ intermartensitic transformation to occur. The measurements reported in this paper indicate that a significant 14M phase fraction (approximately 40%) is introduced during this intermartensitic transformation and remains relatively constant through the transformation.

At the onset of the first plateau, in Fig. 2, the stress–strain curve shows a slight strain softening whereas at the onset of the second plateau the stress levels remain constant. The strain fields indicate that two transformations occur at the first plateau whereas only one occurs at the second plateau. We speculate that the successive nucleation of the 10M and 14M phase is responsible for the strain

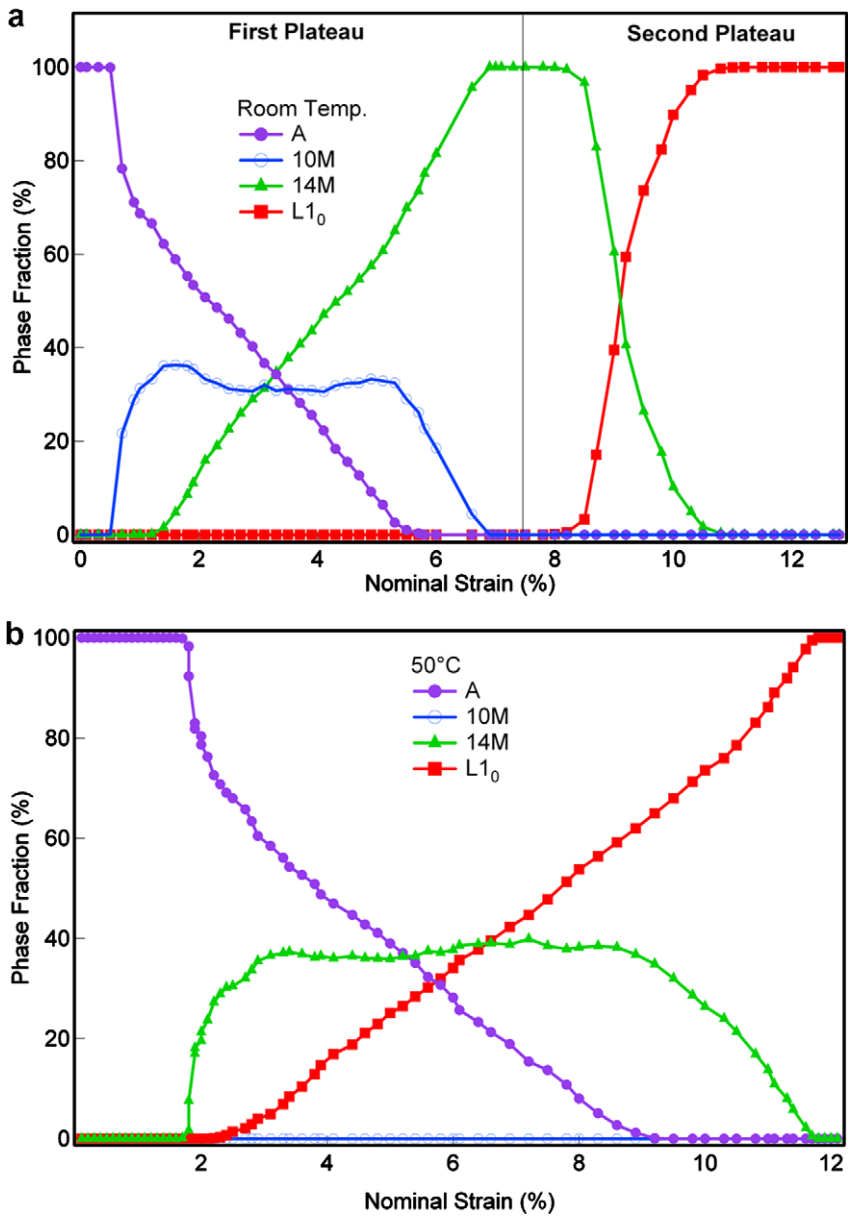

Fig. 5. Evolution of the phase fractions during loading: (a) at room temperature, (b) at 50 °C.

softening along the first plateau. This is rationalized by the following: the strain fields indicate that the 10M phase is nucleated at the critical transformation stress. The 14M phase subsequently transforms only from the 10M phase and does not have to be nucleated from the austenite phase. Thus the martensite-to-martensite transformation (10M → 14M) necessitates a lower stress than that required to nucleate the austenite-to-martensite transformation (A → 10M). This is perhaps expected since the 10M and the 14M phases are both monoclinic structures, and they differ only in their modulation. The phase fraction measurements in Fig. 5a verify that a small fraction of 14M phase is present as early as 1.75% nominal strain. Further along the first plateau, the strain softening regime eventually terminates, and by 5% nominal strain a second stress peak is observed which does not correspond with a nucleation event. Instead, outside the gage section, another 10M transformation band propagates and coalesces with the band within the gage section. Full-field measurements prove valuable in discerning local events influencing the stress–strain curve such as this second stress peak and the strain softening.

The transformation evolution shown by the image sequences during the entire loading and unloading are not identical in Fig. 2. This is most notable during unloading of the second plateau stage where the reverse transformation front appears more diffuse compared to the forward transformation (compare upper and lower right image sequences). The transformation nucleates homogeneously during unloading whereas the transformation nucleates heterogeneously during loading. This indicates that the transformation path is different during loading

and unloading and may contribute to the larger stress hysteresis observed during the second plateau stage. The strain fields during the first plateau stage do not indicate a significant path dependence (compare upper and lower left image sequences), and the stress hysteresis is nearly half of the second plateau stage. This is the first time experiments have documented the magnitude and sequence of the local strain evolution during an intermartensitic transformation and its role on hysteresis.

The interface width for the A → 10M, 10M → 14M, and the A → 14M at 50 °C is significantly narrower than the interface width for the 14M → $L1_0$ transformation. The smaller interface width for the transformation to modulated martensites suggests the deformation is more compatible than the transformation to the tetragonal martensite. Interestingly, the strain varies linearly across the interface. As mentioned earlier, the intermediate modulated martensite phases contain high-density microtwins. These microtwins may serve to minimize the distortion at the austenite and martensite interface. Minimizing the distortion at the interface may also contribute to reducing the stress hysteresis over the first plateau stage. An experimental investigation by Sun and colleagues reported significant distortion at the transformation interface but did not comment on the width of the transition region or how the strain varies within the transition region [20]. Theoretical research by James et al. considers a transition region to accommodate the distortion at an interface [19]. They relate a small transition width to finely twinned martensite. This theoretical work is consistent with our measurements, which indicate a narrower transition width for the modulated martensites compared to the tetragonal martensite. To our knowledge, the present study is the first to report the strain variation within such a transition region.

Comparing the measured local strains to the theoretical transformation strains in Fig. 4, it is apparent that only the 14M phase attains the theoretical maximum strain whereas the 10M and the $L1_0$ phase appear smaller. Since the entire gage section transforms, the smaller measured strains may indicate the formation of multiple CVPs, and/or the lack of detwinning. It is generally accepted that only one CVP forms during stress-induced transformations. Indeed the strain fields indicate a single A/10M interface over the first plateau stage (Fig. 2). It is therefore likely that the 10M phase does not attain the theoretical strain because of limited detwinning. However, in the second plateau stage, the formation of multiple CVPs may not be ruled out since two transformation fronts are observed above 9% nominal strain in Fig. 2. The fronts appear to be inclined approximately +45° and −45° to the applied load which means they most likely contribute equally to the overall transformation strain. Theoretical calculations based on energy minimization [4] indicate that first a CVP strain of approximately 6% is generated, and then an additional detwinning strain of approximately 8%. Since the measured transformation strain of 12% (Fig. 4) is larger than the CVP strain, an incomplete detwinning process may have occurred. The incomplete detwinning process could arise due to the interacting CVPs or due to localized plastic flow.

Full-field strain measurements have allowed the evolution of the phase fractions to be determined during intermartensitic transformations which exhibit multistage and single stage stress–strain curves at 22 °C and 50 °C, respectively. Without such measurements, and based on the stress–strain curve alone, the growth of different martensites and their coexistence would be indistinguishable. This is the first time full-field strain measurements are reported for the entire pseudoelastic loading of a single-crystal. Distinguishing local transformation strains within the multiple phases and characterizing their spatial evolution provides a significant basis for theoretical developments.

5. Summary and conclusions

Experimental results are presented on the multistage transformation behavior of single-crystal NiFeGa with close attention being paid to the full-field strain evolution. Because the intermediate phases are stress-induced, the in situ DIC results provide valuable insight that may not be obtained with other conventional techniques.

The transformation sequence during the multistage stress–strain curve is clarified, showing coexistence of the 10M and 14M phases at room temperature. At a higher temperature, the bypassing of the 10M phase is verified and the transformation to the $L1_0$ phase occurs via the 14M phase. The evolution of the phase fractions were quantified during the pseudoelastic loading at both temperatures. They identified that the intermediate 10M phase fraction at room temperature, and the intermediate 14M phase fraction at 50 °C remain relatively constant during the plateau stages of the transformation.

The evolution of the local strains proved crucial for explaining some of the nuances of the stress–strain curves. The strain softening at the onset of the transformation was rationalized based on the successive nucleation of modulated martensites (10M → 14M). The subsequent increase in stress during the first plateau was identified as a result of interacting martensite bands. The larger stress hysteresis over the second plateau stage was observed in conjunction with a path dependence of the transformation. The strain gradients across the interfaces also supported the larger hysteresis observed over the second plateau stage where the tetragonal martensite is formed. The strain variation across the 14M to $L1_0$ phase is linear and indicates a larger transition width compared to the monoclinic transformations.

Full-field strain measurements provide a tool for exploring the origin of measured strains not reaching theoretical values. This includes identifying whether untransformed domains, multiple martensite variants, and/or incomplete detwinning of martensites are responsible for the smaller measured strains. In NiFeGa, we have identified that the entire material volume transforms, and a combination of

multiple variants and limited detwinning is the cause of smaller measured local and nominal strains.

The results presented in this paper outline details of the evolution of intermartensitic transformations that elucidate the macroscopic stress–strain behavior. These results, obtained from DIC, would prove difficult and in some instances impossible to obtain using other conventional techniques. The DIC technique has far-reaching implications for phase identification, strain measurements, and heterogeneous deformation characterization in new materials displaying complex response.

Acknowledgements

This work was partially supported by the Fracture Control Program, the Midwest Structural Sciences Center (MSSC), and the National Science Foundation CMS-0428428. The MSSC is supported by the US Air Force Research Laboratory Air Vehicles Directorate under contract number FA8650-06-2-3620. The single-crystals were obtained from Prof. Yuri Chumlyakov, Tomsk State University, Russia.

Appendix A. Supplementary data

Supplementary data associated with this article can be found, in the online version, at doi:10.1016/j.actamat.2008.04.033.

References

[1] Kato H, Dutkiewicz J, Miura S. Acta Metall Mater 1994;42:1359.
[2] Sittner P, Novak V, Zárubová N. Acta Mater 1998;46:1265.
[3] Sutou Y, Kamiya N, Omori T, Kainuma R, Ishida K. Appl Phys Lett 2004;84:1275.
[4] Hamilton RF, Sehitoglu H, Efstathiou C, Maier HJ. Acta Mater 2007;55:4867.
[5] Masdeau F, Pons J, Segui C, Cesari E, Dutkiewicz J. J Mag Mater 2006;2043:272.
[6] Efstathiou C, Sehitoglu H, Kurath P, Foletti S, Davoli P. Scripta Mater 2007;57:409.
[7] Daly S, Ravichandran G, Bhattacharya K. Acta Mater 2007;55:3593.
[8] Shaw J, Kyriakides S. J Mech Phys Solids 1995;43:1243.
[9] Shaw J, Kyriakides S. Acta Mater 1997;45:683.
[10] Shaw J, Kyriakides S. Int J Plast 1998;13:837.
[11] Shaw J, Kyriakides S. SPIE 1998;3324:68.
[12] Brinson CL, Schmidt I, Lammering R. J Mech Phys Solids 2004;52:1549.
[13] Brinson CL, Schmidt I, Lammering R. J Intel Mater Syst Struct 2004;13:761.
[14] Pieczyska EA, Gadaj SP, Nowacki WK, Tobushi H. Exp Mech 2006;46:531.
[15] Sittner P, Liu Y, Novak V. J Mech Phys Solids 2005;53:1719.
[16] Hamilton RF, Efstathiou C, Sehitoglu H, Chumlyakov Y. Scripta Mater 2006;54:465.
[17] Chu T, Ranson WF, Sutton MA, Peters WH. Exp Mech 1985;25:232.
[18] Dally JW, Riley WF. Experimental stress analysis. Knoxville, TN: College House Enterprises; 2005. p. 581.
[19] James RD, Hane KF. Acta Mater 2000;48:197.
[20] Sun QP, Zhang XY, Xu Terry T. In: Proceedings of the IUTAM symposium, vol. 25. Bochum, Germany; 1997. p. 407.